Comparison of Interfacial Width of Block Copolymers of d_8-Poly(methyl methacrylate) with Various Poly(*n*-alkyl methacrylate)s and the Respective Homopolymer Pairs as Measured by Neutron Reflection

Jonas Scherble, Bernhard Stark, and Bernd Stühn*

Fakultät für Physik und Institut für Makromolekulare Chemie, Freiburger Materialforschungszentrum, Stefan-Meier-Strasse 21, D-79104 Freiburg i. Br., Germany

Jörg Kressler,* Hendrik Budde, and Siegfried Höring

Fachbereich Werkstoffwissenschaften und Fachbereich Chemie, Martin-Luther-Universität Halle-Wittenberg, D-06099 Halle (Saale), Germany

Dirk W. Schubert

GKSS Forschungszentrum, Max-Planck-Strasse, D-21502 Geesthacht, Germany

Paul Simon and Manfred Stamm

Max-Planck Institut für Polymerforschung, Ackermannweg 10, POB 3148, D-55021 Mainz, Germany

Received April 8, 1998; Revised Manuscript Received December 2, 1998

ABSTRACT: The compatibility of d_8-poly(methyl methacrylate) (d_8-PMMA) and a series of poly(*n*-alkyl methacrylate)s (PnAlkMA) is studied by systematic variation of the length of the *n*-alkyl group from ethyl (EMA) to *n*-pentyl (nPenMA). Simultaneously, a series of symmetric diblock copolymers comprised of d_8-PMMA and of PnAlkMA ranging from ethyl to *n*-hexyl (nHMA) is synthesized. Small-angle X-ray data of bulk samples of d_8-PMMA-*b*-PEMA show that this block copolymer is in the disordered state. A change in the χ over $1/T$ plot occurs between 120 and 130 °C owing to fluctuations. All other block copolymers are in the ordered state at any temperature. The neutron reflection data of d_8-PMMA-*b*-PEMA show a damped cosine concentration depth profile characteristic for thin films of block copolymers in the disordered state. In contrast, the bilayer film of the respective homopolymer pair indicates immiscibility. Neutron reflection measurements on thin films of diblock copolymers ranging from d_8-PMMA-*b*-PnPrMA to d_8-PMMA-*b*-PnHMA and of bilayer films of d_8-PMMA and the respective PnAlkMAs show a decreasing apparent interfacial width with increasing length of the *n*-alkyl group. Taking into account the contributions of capillary waves leads to the inherent interfacial width. By use of the theoretical approach of Matsen and Bates, it is possible to extract the Flory−Huggins χ-parameter between the blocks and the average segment length.

Introduction

The preparation of bilayer films of polymer pairs provides the possibility to study the polymer−polymer interfacial width by appropriate reflection methods.[1] The same methods can be used for thin films of symmetric diblock copolymers forming layers parallel to the surface.[2] The formation of ordered layers in thin films of symmetric diblock copolymers is induced by surface tension differences of the respective blocks. The block with the lower surface tension is enriched on the free surface to air or vacuum. Depending on specific interactions, one of the blocks is enriched on the surface of the substrate.[3] During thermal annealing, the inner parts of the film organize into layers.[4,5] The formation of a layered structure of symmetric block copolymers close to a surface was directly confirmed by microscopic techniques.[6−8] The same phenomenon was studied by reflection methods[2,9] and dynamic secondary mass spectroscopy.[10] Recently, it has been demonstrated theoretically and experimentally that for nonspecific surfaces and for films under confinement an ordering of lamellae perpendicular to the surface can occur.[11−14]

For our studies, block copolymer films were prepared by spin-coating solutions on silicon wafers. Silicon always forms a silicon dioxide layer when in contact with air. Because of the higher polarity of poly(methyl methacrylate) (PMMA) compared to poly(*n*-alkyl methacrylate)s (PnAlkMA) bearing longer alkyl groups, PMMA has more favorable interactions with the silicon dioxide layer. Thus it can be assumed that the PMMA blocks always form the first layer on the substrate. The layers at the interfaces to air and to the substrate have about half the lamella thickness compared to the bulk value.[15] In so-called symmetric films, the same block segregates to both interfaces upon annealing, but in antisymmetric films, each interface adsorbs a different component.[16] In recent years, special emphasis has been given to measurements of the interfacial width between the blocks employing neutron reflection (NR).

To study systematic changes of the interfacial width quantitatively, symmetric diblock copolymers of d_8-poly(methyl methacrylate) (d_8-PMMA) with a homologous series of PnAlkMAs with alkyl groups ranging from ethyl to *n*-hexyl are prepared anionically. The NR data are fitted employing the corresponding scattering length density profiles yielding the apparent interfacial widths and the lamella thickness. In the case of d_8-PMMA-*b*-PEMA the value of the product of the interaction parameter χ and the number of the segments in the polymer N is determined employing small-angle X-ray scattering (SAXS) in the disordered state. Furthermore,

10.1021/ma980547m CCC: $18.00
Published on Web 03/05/1999

Table 1. Characterization of the Homopolymers Used

polymer	d_8-PMMA	PEMA	PnPrMA	PnBMA	PnPenMA	PnHMA
M_n (kg mol^{-1})	33.0	19.5	16.7	22.9	17.9	15.9
M_w/M_n	1.04	1.01	1.01	1.01	1.01	1.01

Table 2. Characterization of the Block Copolymers Used[a]

PnAlkMA-*b*-d_8-PMMA	PEMA	PnPrMA	PnBMA	PnPenMA	PnHMA
M_n PMMA [kg mol^{-1}]	19.6	16.7	22.8	19.5	19.4
M_n PnAlkMA [kg mol^{-1}]	19.5	16.7	22.9	17.6	15.9
M_w/M_n overall	1.05	1.04	1.06	1.04	1.07
f	0.49	0.46	0.43	0.38	0.34

[a] f is the number fraction of statistical segments of PnAlkMA blocks in the copolymer.

Table 3. Degree of Polymerization of d_8-PMMA N_{PMMA} and of PnAlkMA $N_{PnAlkMA}$, Apparent Interfacial Width a_{app}, Intrinsic Interfacial Width a_I, and Lamella Thickness D_{lam} of the Block Copolymers[a]

d_8-PMMA-*b*-PnAlkMA	PnPrMA	PnBMA	PnPenMA	PnHMA
annealing	11.5 h, 156 °C	13 h, 140 °C	14 h, 140 °C	13.5 h, 130 °C
$N_{PnAlkMA}$	130	161	113	93
N_{PMMA}	155	211	181	180
D_{lam} [nm]	20.7	23.6	23.4	26.8
a_{app} [nm]	4.4	4.0	3.0	3.4
a_I [nm]	4.0 ± 1.7	3.5 ± 1.9	2.3 ± 2.6	2.8 ± 2.2
χ	0.063 ± 0.029	0.062 ± 0.036	0.12 ± 0.19	0.12 ± 0.13
b [nm]	0.76 ± 0.12	0.72 ± 0.16	0.72 ± 0.29	0.87 ± 0.33

[a] The values of the interaction parameter χ and the average segment lengths b obtained according to Matsen and Bates[37] are also shown.

bilayer films of d_8-PMMA and the respective homologous series of poly(*n*-alkyl methacrylate) homopolymers are investigated by NR. A comparison of the interfacial width data of the block copolymers and the respective homopolymer pairs is done and takes into account contributions of capillary waves.

Experimental Section

Materials. Tetrahydrofuran (THF, Aldrich) was freshly distilled over sodium/benzophenone (purple) under argon after refluxing for 8 h. The monomers (all from Polysciences) ethyl methacrylate (EMA), *n*-propyl methacrylate (nPrMA), *n*-butyl methacrylate (nBMA), *n*-pentyl methacrylate (nPenMA), *n*-hexyl methacrylate (nHMA), and deuterated methyl methacrylate (d_8-MMA, Promochem) were purified by washing with 3% NaOH solution to remove inhibitor prior to stirring with CaH_2 for 48 h. The dried monomers were finally vacuum-distilled under argon and stored at −20 °C. Prior to use, all monomers were titrated with 17% Et_3Al solution in *n*-hexane (Merck) until a greenish color appeared and again vacuum-distilled under argon. *sec*-Butyllithium (*sec*-BuLi, Aldrich) in cyclohexane was used as received. 1,1-Diphenylethylene (DPE, Aldrich) was distilled under argon, titrated with *sec*-BuLi until a red color appeared, and again distilled. Lithium chloride (LiCl, Fluka) was dried under high vacuum ($<10^{-5}$ Torr) at 120 °C and kept under argon in freshly distilled THF.

Polymer Synthesis. Syntheses were carried out by the syringe technique under dry argon in a glass reactor equipped with an inlet for argon/vacuum and a septum. The undeuterated polymer was always polymerized first. The second block was synthesized using the deuterated MMA. The initiator (3-methyl-1,1-diphenylpentyl)lithium was generated in the reactor before the addition of monomer. A typical example for the polymerization procedure is given below. The LiCl solution (10 equiv LiCl to initiator) was filled into the reactor. After that, THF was added, followed by the addition of DPE (2 equiv to the amount of *sec*-BuLi needed for the preparation of the initiator). After titration with a few drops of *sec*-BuLi (until a stable red color appeared), the calculated amount of *sec*-BuLi was added, and the mixture was cooled to −78 °C. Within 1 min, the undeuterated monomer was added under strong stirring, and the mixture was stirred for 15 min. Then the deuterated MMA monomer was added within 1 min. After being stirred for 1 h, the polymerization was stopped with methanol. The respective poly(*n*-alkyl methacrylate) homopolymers were obtained by carrying out the synthesis under identical conditions. Both the homopolymer and the block copolymer were isolated by precipitation in a 10 fold excess of methanol/water (70/30). Samples were filtered and dried in a vacuum at 25 °C for several hours. The molecular weights were determined by size exclusion chromatography (Waters) with THF as eluant. A styragel HT-4 column was used. Calibration was done with poly(methyl methacrylate) standards (Polymer Standards Service). All molecular weight data are given in Tables 1 and 2.

Table 4. Apparent Interfacial Width a_{app} and Intrinsic Interfacial Width a_I of the Bilayer Films of d_8-PMMA and PnAlkMA after Annealing

bottom layer	PEMA	PnPrMA	PnBMA	PnPenMA
annealing	10 h, 132 °C	10 h, 132 °C	10 h, 132 °C	3 h, 124 °C
a_{app} [nm]	6.1	4.4	4.1	3.9
a_I [nm]	5.2 ± 2.0	3.0 ± 3.1	2.7 ± 3.5	2.3 ± 4.0

Spin-Coating of Block Copolymer Films. Thin films of the block copolymers were prepared by spin-coating[17] of 3 wt % solutions of polymer in chlorobenzene on silicon wafers at 3000 rpm. The thickness of the films varied between 55 and 70 nm. The film thickness was independently confirmed by X-ray reflection and by using an alpha stepper (alpha step 300). All films were dried in a vacuum oven for several days and then isothermally annealed as indicated in Table 3. The d_8-PMMA-*b*-PEMA film was annealed at 150 °C for 12 h. The surface roughness of the films was smaller than 1 nm (RMS value), as measured by X-ray reflection and phase interference microscopy.

Bilayer Films. The bottom film was spin-coated directly on the silicon wafer. The top film was spin-coated onto a glass substrate, floated off onto a water surface, and picked up with the bottom film on the substrate. The films were dried under vacuum and were annealed as indicated in Table 4.

Neutron Reflection. Measurements were carried out on the TOREMA-2 neutron reflectometer at GKSS, Geesthacht, Germany. The neutrons are monochromatized by Bragg reflection from a graphite crystal under an angle of 39°. In this way, neutrons of 0.43 nm wavelength are selected. The neutrons are collimated by two slits in a distance of $l = 1740$ mm. The widths of the slits are $b_1 = 0.7$ and $b_2 = 0.45$ mm. So the geometrical divergence $\Delta\theta_{geom}$ of the beam can be calculated to be $\Delta\theta_{geom} = 0.04°$. From geometrical considerations, it is

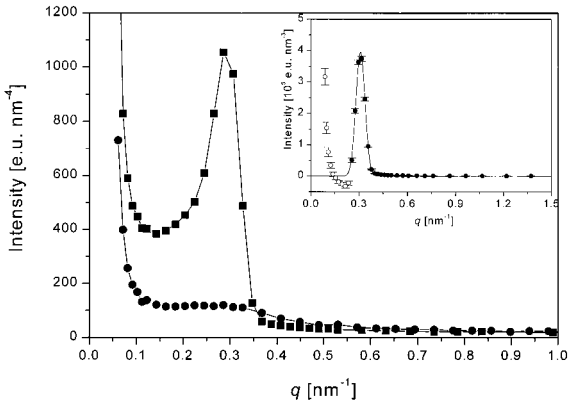

Figure 1. Smeared SAXS data of d_8-PMMA-*b*-PEMA taken at 100 °C (circles). For comparison, the data of d_8-PMMA-*b*-PnPrMA also taken at 100 °C are added (squares). The lines are drawn to guide the eye. The inset shows the desmeared data of d_8-PMMA-*b*-PnPrMA. The line represents the best fit of a Gaussian to the data drawn in full circles.

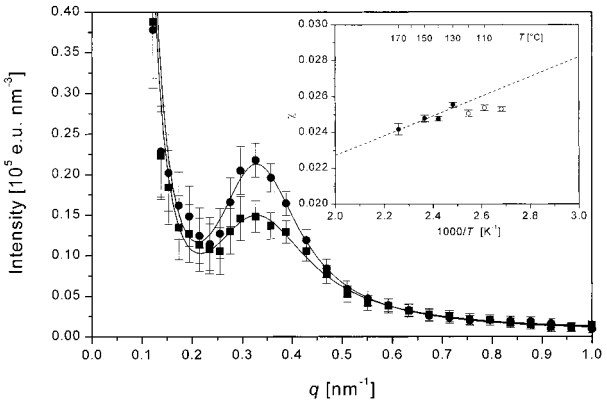

Figure 2. Desmeared SAXS data of d_8-PMMA-*b*-PEMA taken at 130 °C (circles) and 170 °C (squares). The lines represent the best fit of the correlation function of the disordered state to the data. The inset shows χ over 1000/T. The dashed line represents the linear best fit of the data drawn in full circles.

seen that not the whole beam will be reflected by the specimen at low angles. With typical sample sizes of about 10 × 10 cm, the whole beam will be reflected if the sample angle $\theta > 0.4°$ ($q > 0.20$ nm^{-1}). For this reason, the reflectivity in the total reflection regime ($\theta < \theta_c \approx 0.3°$) appears to be lower than 1, and the data in this regime are not taken into consideration. All measurements were carried out after quenching to room temperature in an angular range of $0.1° < \theta < 1.8°$ corresponding to scattering vectors $q = (4\pi/\lambda) \sin\theta$ of $0.05 < q/(\text{nm}^{-1}) < 0.9$.

By use of a matrix formalism,[18] the reflection curves can be calculated from the scattering length density profile in the direction perpendicular to the interfaces. Minimizing the deviation between calculated and experimental reflection curves thus yields essential parameters for the scattering length density profile like film thickness, lamella spacing, and apparent interfacial width.

Small-Angle X-ray Scattering (SAXS). The sample was placed in an evacuated tool and heated to the melt. Then it was pressed to yield a homogeneous block of 2 mm thickness. The sample was then slowly cooled to room temperature and placed in an evacuated compact Kratky camera (PAAR). The scattering experiments use the radiation from a sealed X-ray tube with copper anode and a Siemens generator (Kristalloflex 710H). A primary monochromator selects a wavelength of Cu Kα of $\lambda = 0.154$ nm. The accessible range of scattering vectors is $0.1 < q/(\text{nm}^{-1}) < 5$. The scattered intensity is recorded with a scintillation counter in step-scanning mode. Because of the slitlike cross section of the primary beam in this setup, the scattered intensity at one angle contains a certain range of scattering vectors. This problem is solved by desmearing the data using standard methods.[19] Moreover, the data are put on an absolute scale by using the moving slit device (PAAR) to determine the flux of the primary beam. The resulting intensity is the scattering cross section per volume in units of the Thompson cross section.

Results and Discussion

***d_8*-PMMA-*b*-PEMA and *d_8*-PMMA-*b*-PnPrMA in Bulk.** To obtain information on the microphase behavior of the block copolymers under investigation, SAXS measurements are carried out. Assuming a continuous increase of incompatibility between PMMA and *n*-alkyl methacrylates with increasing *n*-alkyl length, we have studied the bulk structure of their diblock copolymers. The composition of the block copolymers is nearly symmetric (see Table 2). We therefore expect a lamellar type of ordering. In Figure 1, we compare the SAXS profile obtained in Kratky geometry for d_8-PMMA-*b*-PEMA with that obtained for d_8-PMMA-*b*-PnPrMA. The samples were slowly cooled from 170 to 100 °C. A qualitatively different scattering behavior is seen in this figure. The d_8-PMMA-*b*-PnPrMA exhibits a strong, narrow peak whereas the intensity of the weak maximum found for d_8-PMMA-*b*-PEMA is an order of magnitude smaller. This difference is not due to the difference in scattering contrast. The electron density difference is $\Delta\eta = 0.010$ mol e/cm^3 for d_8-PMMA-*b*-PEMA and $\Delta\eta = 0.019$ mol e/cm^3 for d_8-PMMA-*b*-PnPrMA. Closer inspection of the scattering profiles shows that they also differ with respect to their detailed form.

After desmearing, in the case of d_8-PMMA-*b*-PnPrMA, we find a symmetric peak which is well fitted with a Gaussian, as is demonstrated in the inset of Figure 1. The maximum is at $q = 0.31$ nm^{-1}. No higher order maxima are present. This is in accordance with the expected lamellar structure as the second-order maximum is suppressed in the case of equal thickness of the two layers constituting a period. The period or lamella thickness then is 20.3 nm. This compares well with the value found from neutron reflection measurements on films of the same sample (see below).

The d_8-PMMA-*b*-PEMA diblock copolymer does not show such a high degree of order. In Figure 2, we display desmeared SAXS data at two temperatures (130 °C and 170 °C). The broad asymmetric peak decreases in intensity with increasing temperature. This behavior is well-known for block copolymers in their disordered state, and it has been studied in great detail in recent years following the work of Leibler.[20] Concentration fluctuations in the disordered melt give rise to the scattering and the structure factor $N/S(q)$ is calculated on the basis of the structure factor of the noninteracting system and the interaction described in terms of the Flory−Huggins parameter χ. Using this result and taking polydispersity of the polymer into account,[21] we are able to arrive at a good fit to our data. These results are included in Figure 2 as the full curves. The important result for our study is the value of the interaction parameter χN which we may thus extract from the data. It may be reduced to the value of χ using the degree of polymerization $N = 350$. The inset of Figure 2 shows the variation of χ with temperature. The deviation from the expected linear dependence on $1/T$ is due to concentration fluctuations in the disordered state.[22] They enable a partial separation of the different monomers without the loss of entropy that is encoun-

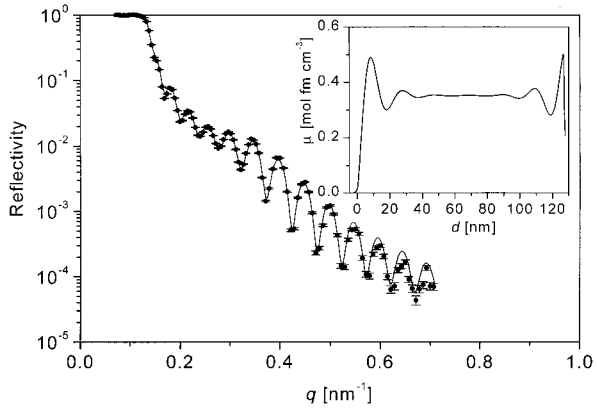

Figure 3. NR trace of a thin film of d_8-PMMA-*b*-PEMA after isothermal annealing for 12 h at 150 °C. The full line represents the best fit to the data. The inset shows the scattering length density profile used for the data fit.

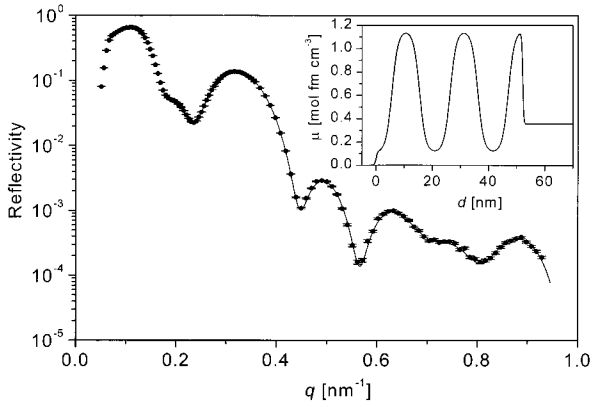

Figure 4. NR trace of the thin film of d_8-PMMA-*b*-PnPrMA after isothermal annealing for 12 h at 150 °C. The full line represents the best fit to the data. The inset shows the scattering length density profile used for the data fit.

tered when the system transforms into the ordered state. This effect[22,23] modifies the scattering function so that the interaction parameter is only an apparent one which is smaller than the intrinsic interaction. Scattering experiments[24,25] have confirmed this expectation. The intrinsic interaction is therefore only seen at high T. Thus only the high-temperature data in the inset of Figure 2 drawn in full circles are approximated by $\chi = A/T + B$ and we find $A = 5.5 \pm 1.4$ K and $B = 0.012 \pm 0.004$. As a result of these measurement on the bulk structure, we find that the block copolymer d_8-PMMA-*b*-PnPrMA is in the ordered state and forms lamellae. The block copolymer d_8-PMMA-*b*-PEMA is in the disordered state at all temperatures under investigation.

***d*$_8$-PMMA-*b*-PEMA in Thin Films.** In comparison to the other block copolymers under investigation, the d_8-PMMA-*b*-PEMA exhibits a different reflection pattern. There are not distinct layers, as expected from a fully microphase-separated system confined in thin films, but there are concentration waves initiated at the free surface and the interface to the substrate. The concentration waves are damped, and finally, a mean scattering length density in the middle of the film is observed. This behavior was first found by Menelle et al.[26] Figure 3 shows the reflection curve and the corresponding scattering length density profile perpendicular to the surface of the film. The scattering length density profile $\mu(z)$ can be described by a damped cosine function

$$\mu(z) = \mu_e e^{-z/\xi} \cos\left(2\pi\frac{z}{L} + \phi_0\right) + \mu_0 \qquad (1)$$

where μ_e is the excess surface concentration, ξ is the correlation length, z is the distance from the surface, L is the period, ϕ_0 the phase shift, and μ_0 is the average concentration. Theoretical arguments of Fredrickson lead to a depth-dependent concentration profile expression similar to that of eq 1 where ξ and L are given by[24]

$$\xi = \sqrt{2}/q^*(1 - \bar{\chi}/\bar{\chi}_S) \qquad (2)$$

and

$$L = \sqrt{2}2\pi/q^*(1 + \bar{\chi}/\bar{\chi}_S)^{-1/2} \qquad (3)$$

where , $\bar{\chi}_S = 3^{1/2}/[f(1-f)]^{3/2}$, $\bar{\chi} = 2\chi N - 2(\chi N)_S + \bar{\chi}_S$, and $(\chi N)_S = 10.495$ is the value of χN at the spinodal for $f = 0.5$ according to Leibler.[20] χN and q^* have been previously measured by SAXS. f is the number fraction of statistical segments of PnAlkMA blocks in the copolymer. Substitution of these quantities in eqs 2 and 3 yields $L = 20.4$ nm and $\xi = 8.9$ nm, which are in good agreement with experimental results obtained by NR, where $L = 19.5$ nm and $\xi = 9.6$ nm from both interfaces.

***d*$_8$-PMMA-*b*-PnPrMA, *d*$_8$-PMMA-*b*-PnBMA, *d*$_8$-PMMA-*b*-PnPenMA, and *d*$_8$-PMMA-*b*-PnHMA Thin Films.** All of these films exhibited a similar neutron reflection profile and scattering length density profile as shown for d_8-PMMA-*b*-PnPrMA in Figure 4. The reflection curves were fitted using models for the scattering length density profiles. The interfaces between the substrate and the film, the film and the vacuum, and between the single lamellae were described by error functions. The width of the interface is given by the standard deviation σ. From this, an interfacial width can be calculated using $a_{app} = (2\pi)^{1/2}\sigma$.[27] The theoretical reflection curves were calculated by the matrix method.[28] During the fitting procedures, the parameter of the roughness of the free surface was held constant at a value of 1.0 nm, as determined by X-ray reflection measurement. The resulting lamella sizes and the interfacial widths are given in Table 3. It can be seen that the interfacial width decreases with increasing *n*-alkyl chain length, as is expected because of the lower polarity of the *n*-alkyl methacrylates with longer *n*-alkyl chains. In the past, several groups[29−31] illustrated that capillary waves have a significant effect on the measured interfacial width, which is therefore called an apparent interfacial width. Capillary waves can be described as the mean square displacement of the interface $\langle(\Delta z)^2\rangle$ from its ideal position at $z = 0$. The theory of interfacial fluctuations was developed to describe capillary waves at the liquid/vapor interface.[32,33] Extension of these theories to polymeric systems leads to[29]

$$\langle(\Delta z)^2\rangle = \frac{k_B T}{2\pi\gamma_{ab}} \ln\left(\frac{\lambda_{max}}{\lambda_{min}}\right) \qquad (4)$$

where γ_{ab} is the interfacial tension between the polymers and λ_{max} and λ_{min} are the maximum and minimum wavelengths of the fluctuations. We expect the lower wavelength limit λ_{min} to be in the range of the intrinsic

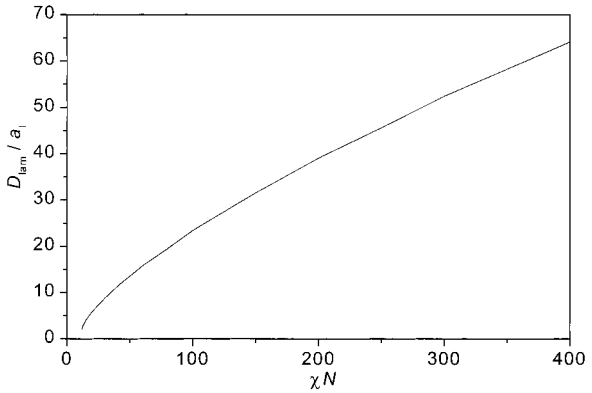

Figure 5. Dependence of D_{lam}/a_I on χN according to Matsen and Bates.[37]

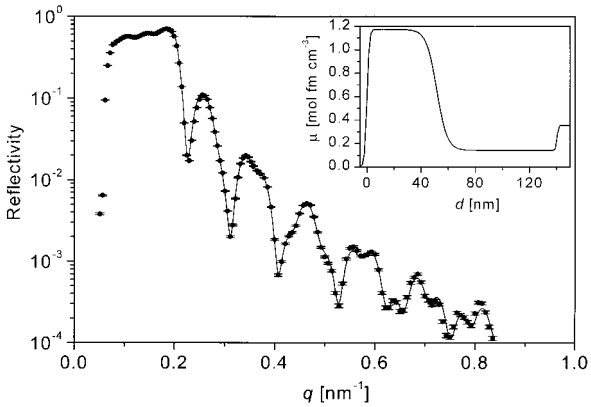

Figure 6. NR traces of the bilayer film of d_8-PMMA and PEMA taken after isothermal annealing for 10 h at 132 °C. The full line represents the best fit to the data. The inset shows the scattering length profile used for the data fit.

interfacial width. For block copolymers, the lamella thickness D_{lam} provides a good estimate of λ_{max}.[29] Fluctuations with longer wavelengths force the molecules to be stretched resulting in additional elastic energy, so these fluctuations will be suppressed. Note that because of the logarithm in eq 4 a comparably large error in estimating the ratio $\lambda_{max}/\lambda_{min}$ only results in a small deviation of the value of fluctuations. The interfacial tension for infinite molar mass is given by[34]

$$\gamma_{ab} = b\rho_0 k_B T(\chi/6)^{1/2} \quad (5)$$

where $1/\rho_0$ is the volume per monomeric unit, which is 0.135 nm^3 in the case of PMMA. Because the block copolymers with alkyl groups longer than ethyl are phase-separated, their interaction parameters should be well above the ODT given in a rough estimation by $(\chi N)_S = 10.495$. With $N \approx 370$ this leads to $\chi > 0.03$. We assume a value of $\chi = 0.07 \pm 0.02$ for the interaction parameter between PMMA and the PnAlkMAs. For the segment length b, we use the value of PMMA, 0.75 nm.[35,36] So at 130 °C, the interfacial tension will be $\gamma_{ab} = 2.5 \pm 1.0$ mJ/cm^2, which is a suitable value for immiscible polymers. For the intrinsic interfacial width we assume $a_{int} = \lambda_{min} = 3$ nm. From the measurements, we take $D_{lam} = \lambda_{max} \approx 25 \pm 0.5$ nm. This results in a mean square displacement of the interface of $\langle(\Delta z)^2\rangle^{1/2} = 0.75 \pm 0.89$ nm. The mean square displacement is related to the fluctuation contribution of the interface a_{fluct} by a factor of $2(\pi)^{1/2}$, so $a_{fluct} = 1.9 \pm 2.2$ nm. The experimental results of the interfacial width a_{app} are corrected according to the fluctuations using $a_I = (a_{app}^2 - a_{fluct}^2)^{1/2}$. The values are given in Table 3. It can be seen that the apparent interfacial width must be reduced by approximately 0.6 nm in order to obtain the intrinsic interfacial width.

The data were evaluated according to Matsen and Bates[37] who applied a full mean field theory. Matsen and Bates provided two curves, one relating the lamella size D_{lam} normalized to the end-to-end distance bN^2 over χN and the other relating the normalized intrinsic interfacial width a_I over χN. By dividing these two curves, one can obtain the curve shown in Figure 5, which describes the relationship of D_{lam}/a_I and χN, which is independent of the segment length. From experimental values, D_{lam}/a_I is calculated, and χN is determined. By use of the curves of Matsen and Bates the value of a_I/bN^2 or D_{lam}/bN^2 can be calculated from χN. From these, the value of the average segment length b can be determined using the experimental values of a_I or D_{lam}, respectively. The resulting values of the interaction parameters χ and the average segment lengths b are listed in Table 3. The values of χ increase with the length of the *n*-alkyl group of PnAlkMA, as is expected for the growing incompatibility of d_8-PMMA and PnAlkMA. However, the errors in determining the interaction parameter and the average segment length from the intrinsic interfacial width are large because of the large errors in estimating the fluctuation contribution of a_{app}.

***d*$_8$-PMMA/PnAlkMA Bilayer Films.** A typical example of the reflection profile and of the scattering length density profile of these films is given in Figure 6. The apparent interfacial widths between d_8-PMMA and PnAlkMA are listed in Table 4. To obtain the intrinsic interfacial width, the fluctuation contribution again has to be accounted for. The estimation of the interfacial tension is the same as for the block copolymers. However, the upper wavelength limit of the fluctuations λ_{max} has to be rethought: Because there is no periodic lamellar structure of the film, there is no stretching of the chains due to fluctuations of the interface. Thus, the upper wavelength limit is determined by the lateral coherence length for the neutron reflectivity measurement, which is approximately 1 μm.[29] The contribution of the fluctuations to the interfacial width of the bilayer films obtained from eq 4 is $a_{fluct} = 1.9 \pm 2.2$ nm. As a result of the larger cutoff length, the capillary wave contribution to the interfacial width is approximately double that of the block copolymers. In Table 4, the values of the interfacial width are corrected according to the capillary wave broadening. Obviously, the values of a_I found for the bilayer films are lower than those found for the block copolymers. Sferazza et al.[31] showed that for bilayer films comprised of a d_8-polystyrene layer on top of a PMMA film both dispersive forces across the film and the neutron coherence length limit the upper wavelength of the fluctuations: Up to layer thicknesses of 100 nm, a logarithmic relationship between the layer thickness and the apparent interfacial width due to dispersive forces is found. For thicker layers, the wavelength of the fluctuations becomes too large to be dissolved in the reflectivity experiment, and the interfacial width becomes independent of the film thickness. The bilayer films under consideration in this work have a d_8-PMMA layer of about 50 nm on top of a PnAlkMA film of approximately 100 nm thickness. The apparent interfacial width of these films might still depend on the film thickness, so

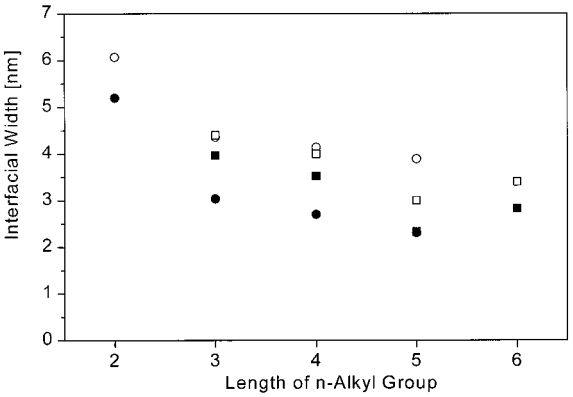

Figure 7. Intrinsic interfacial width a_I (full symbols) and apparent interfacial width a_{app} (open symbols) of block copolymers of d_8-PMMA with different *n*-alkyl methacrylates as a function of the length of the *n*-alkyl chain (circles). The data of the corresponding bilayer films using the respective homopolymer pairs are also shown (squares).

taking the neutron coherence length as an upper limit might cause an overestimation of the capillary wave contribution leading to a smaller value of the intrinsic interfacial width. However, the bilayer films exhibit the same tendency of the interfacial width as the block copolymers. The interfacial width decreases as the length of the alkyl group is increased. The comparison of the intrinsic interfacial width shows that the block copolymers have a lower interfacial roughness than the respective homopolymer pairs.

Conclusion

It was shown by SAXS measurements that the block copolymer d_8-PMMA-*b*-PEMA is in the disordered state. This is in agreement with NR data showing a damped cosine concentration profile. According to Semenov, the influence of the waviness of the interfaces in block copolymer microphases on the apparent interfacial width is relatively small.[29] On the other hand, Sferazza et al. found a strong contribution of the capillary waves to the apparent interfacial widths between homopolymers.[31] This contribution depends on the film thickness and cannot be neglected. In Figure 7, the intrinsic interfacial widths and the apparent interfacial widths, respectively, of the homopolymer films and of the respective block copolymer films are plotted against the length of the *n*-alkyl side chain. It appears that the fitting parameter a_{app} is very similar for block copolymers and the respective homopolymer pairs. It is assumed that the contribution of capillary waves to the apparent interfacial width are less in block copolymers compared to the homopolymer pairs because of different cutoff lengths in the experiments. This leads finally to the result that the intrinsic interfacial width of block copolymers is greater than that of the respective homopolymer pairs. The interfacial widths of both the homopolymers and the block copolymers decrease with increasing *n*-alkyl chain length of the PnAlkMAs. The interaction parameter was determined from the interfacial widths of the block copolymers. As expected for the decreasing chemical compatibility of PnAlkMA with longer *n*-alkyl chains with PMMA, the χ-parameters increase.

Acknowledgment. The authors thank B. Heck for kind assistance with SAXS measurements. J.K., H.B., and S.H. thank the Deutsche Forschungsgemeinschaft for support (Innovationskolleg − Neue Polymermaterialien). This work has been supported by the BMBF (Grant Number 03-ST4FRAU-0).

References and Notes

(1) Stamm, M. *Adv. Polym. Sci.* **1992**, *100*, 357.
(2) Russell, T. P. *Mater. Sci. Rep.* **1990**, *5*, 171.
(3) Anastasiadis, S. H.; Russell, T. P.; Satija, S. K.; Majkrzak, C. F. *Phys. Rev. Lett.* **1989**, *62*, 1852.
(4) Mayes, A. M.; Russell, T. P.; Bassereau, P.; Baker, S. M.; Smith G. S. *Macromolecules* **1994**, *27*, 749.
(5) Mutter, R.; Stühn, B. *Macromolecules* **1995**, *28*, 5022.
(6) Vanzo, Ed. *J. Polym. Sci., Part A* **1966**, *4*, 1727.
(7) Kovacs, A. J. *Chim. Ind., Genie Chim.* **1967**, *97* (3), 315.
(8) Hasegawa, H.; Tanaka, H.; Yamasuki, K.; Hashimoto, T. *Macromolecules* **1987**, *20*, 1651.
(9) Anastasiadis, S. H.; Russell, T. P.; Satija, S. K.; Majkrzak, C. F. *J. Chem. Phys.* **1990**, *92*, 5677.
(10) Russell, T. P.; Coulon, G.; Deline, V. R.; Miller, D. C. *Macromolecules* **1989**, *22*, 4600.
(11) Matsen, M. W. *J. Chem. Phys.* **1997**, *106*, 7781.
(12) Pickett, G. T.; Balazs, A. C. *Macromolecules* **1997**, *30*, 3097.
(13) Russell, T. P.; Lambooy, P.; Kellogg, G. J.; Mayes, A. M. *Physica B* **1995**, *213&214*, 22.
(14) Mansky, P.; Russell, T. P.; Hawker, C. J.; Pitsikalis, M.; Mays, J. *Macromolecules* **1997**, *30*, 6810.
(15) Hasegawa, H.; Hashimoto, T. *Macromolecules* **1985**, *18*, 589.
(16) Kellog, G. J.; Walton, D. G.; Mayes, A. M.; Lambooy, P.; Russell, T. P.; Gallagher, P. D.; Satija, S. K. *Phys. Rev. Lett.* **1996**, *76*, 2503.
(17) Schubert, D. W. *Polym. Bull.* **1997**, *38*, 177.
(18) Lekner J. *Theory of Reflection*; Martinus Nijhoff: Dordrecht, Netherlands, 1987.
(19) Strobl, G. *Acta Crystallogr.* **1970**, *A26*, 367.
(20) Leibler, L. *Macromolecules* **1980**, *13*, 1602−17.
(21) Holzer, B.; Lehmann, A.; Kowalski, M.; Stühn, B. *Polymer* **1991**, *11*, 1935.
(22) Fredrickson, G. H.; Helfand, E. *J. Chem. Phys.* **1987**, *87*, 697.
(23) Fredrickson, G. H. *Macromolecules* **1987**, *20*, 2535.
(24) Stühn, B.; Mutter, R.; Albrecht, T. *Europhys. Lett.* **1992**, *18*, 427.
(25) Bates, F. S.; Rosedale, J. H.; Fredrickson, G. H.; Glinka, G. J. *Phys. Rev. Lett.* **1988**, *61*, 2229.
(26) Menelle, A.; Russell, T. P.; Anastasiadis, S. H.; Satija, S. K.; Majkrzak, C. F. *Phys. Rev. Lett.* **1992**, *68*, 67.
(27) Russell, T. P.; Hjelm, R. P.; Seeger, P. A. *Macromolecules* **1990**, *23*, 890.
(28) Penfold, J.; Thomas, R. K. *J. Phys.: Condens. Matter* **1990**, *2*, 1369.
(29) Semenov, A. N. *Macromolecules*, **1993**, *26*, 6617.
(30) Shull, K. R.; Mayes, A. M.; Russell, T. P. *Macromolecules*, **1993**, *26*, 3929.
(31) Sferazza, M.; Xiao, C.; Jones, R. A. L.; Bucknall, D. G.; Webster, J.; Penfold, J. *Phys. Rev. Lett.* **1997**, *78* (19), 3693.
(32) Buff, F. P.; Lovett, R. A.; Stillinger, F. H. *Phys. Rev. Lett.* **1965**, *15*, 621.
(33) Rowlinson, J.; Widom, B. *Molecular Theory of Capillarity*; Oxford University Press: Oxford, U.K., 1982.
(34) Helfand, E.; Sapse, A. M. *J. Chem. Phys.* **1975**, *62*, 1327.
(35) Kirste, R. G.; Kratky, O. *Z. Phys. Chem. (Munich)* **1962**, *31*, 383.
(36) Kirste, R. G. *Makromol. Chem.* **1967**, *101*, 81.
(37) Matsen, M. W.; Bates, F. S. *Macromolecules* **1996**, *29*, 1091.

MA980547M